OAK RIDGE NATIONAL LABORATORY

operated by

UNION CARBIDE CORPORATION
NUCLEAR DIVISION
for the
U.S. ATOMIC ENERGY COMMISSION

ORNL - TM - 2421

COPY NO. - 66

DATE - November 14, 1968
UC-80 - Reactor Technology

DESIGN CURVES FOR BURNOUT HEAT FLUX IN FORCED-CONVECTION SUBCOOLED LIGHT-WATER SYSTEMS

W. R. Gambill

Design (minimum) values of burnout heat flux for subcooled water systems were calculated with the writer's superposition correlation. The calculated fluxes were not reduced with an arbitrary design factor; instead, each term was modified to coincide with the lower bound of available experimental data — i.e., established scatter limits were applied to each factor separately. Burnout fluxes were plotted for $10 < V < 100$ fps, $15 < P < 3000$ psia, $100 < \Delta t_{sub} < 400$°F, and channel equivalent diameters of 0.1 and 0.5 in.

In addition, a simple method is described for estimating the ratio of burnout to incipient-boiling heat fluxes. The method is applied to the HFIR to indicate the dependence of the subject flux ratio on velocity, subcooling, and pressure.

Printed in the United States of America. Available from Clearinghouse for Federal Scientific and Technical Information, National Bureau of Standards, U.S. Department of Commerce, Springfield, Virginia 22151
Price: Printed Copy $3.00; Microfiche $0.65

CONTENTS

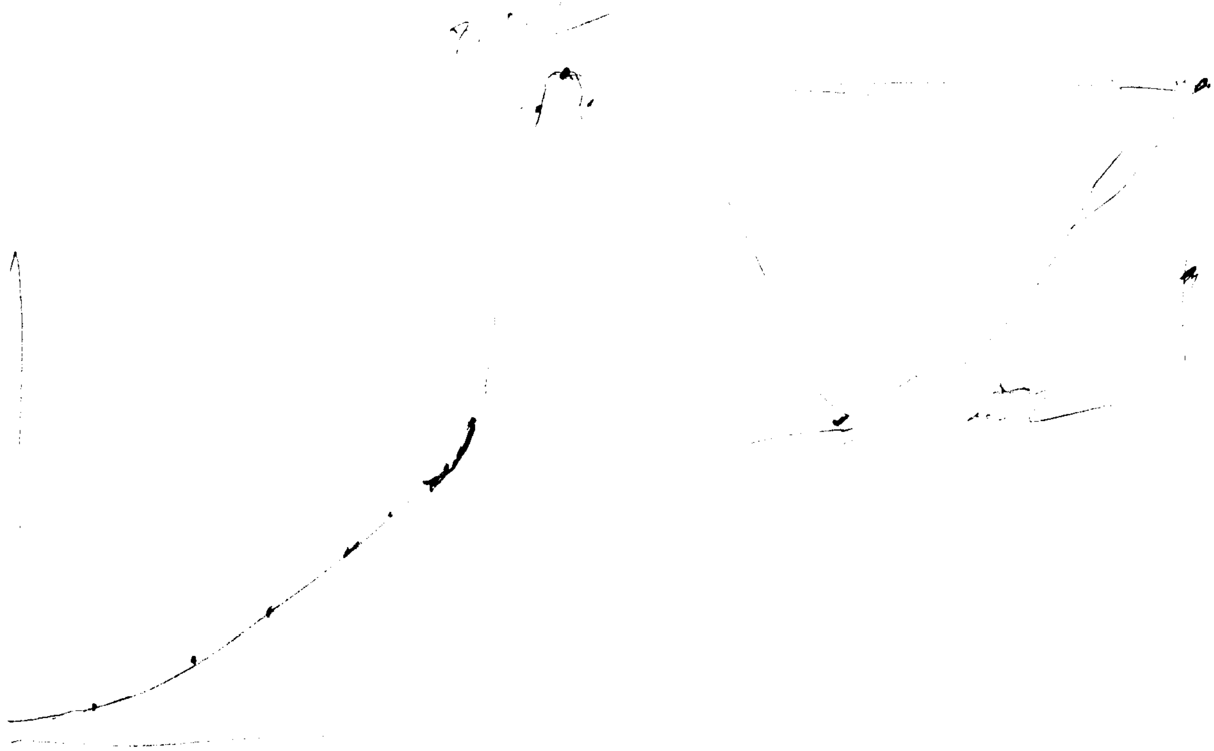

INTRODUCTION

The recurring need for estimates of burnout (critical) heat fluxes in subcooled water systems prompted the writer to prepare a group of curves with which rapid estimates may be made for purposes of initial evaluation or preliminary design. The calculations were made with an additive or superposition correlation[1] which has been shown to be in better accord with burnout data for subcooled coolants (~1400 points) than other correlations.

In the additive method, the burnout flux is taken to be the sum of a term characterizing the boiling contribution in the absence of forced convection and another term representing the forced-convection contribution in the absence of boiling. In the original proposal,[1] predictions of the correlation were compared with data for seven coolants in axial, swirl, and cross flow in tubular, annular, rectangular, and rod geometries over broad ranges of flow conditions ($0.05 < V < 174$ fps, $4.2 < P < 3000$ psia, and $0 < \Delta t_{sub} < 506°F$) which resulted in burnout fluxes from 0.1×10^6 to 37.4×10^6 Btu/hr•ft^2. It was shown that 96% of the representative data (~900 tests) agreed with the predictions within a maximum deviation of 40%. Using burnout data for water only, the additive correlation encompassed ~35% more points at a maximum deviation level of 40% than did Bernath's well-known correlation[2] for subcooled flow burnout.

The superposition correlation is expressed by:

$$\phi_{bo} = (\phi_{bo})_{boil} + (\phi_{bo})_{nb} \quad , \tag{1}$$

in which

$$(\phi_{bo})_{boil} = (\phi_{bo})_{pool} = (\phi_{bo})_{pool,sat}\, F_{sub} \quad , \tag{2}$$

and where

$$F_{sub} \equiv \left[\frac{(\phi_{bo})_{sub}}{(\phi_{bo})_{sat}}\right]_{pool} \quad . \tag{3}$$

The saturated pool term was evaluated with the Kutateladze-Zuber equation:

$$(\phi_{bo})_{pool,sat} = K\lambda\rho_v^{1/2}(\sigma g_c a\Delta\rho)^{1/4} \quad , \tag{4}$$

and the subcooling factor was calculated, in the original version,[1] with a relation proposed by Kutateladze on the basis of limited small-wire data:

$$F_{sub} = 1 + \left(\frac{\rho_\ell}{\rho_v} \right)^{0.923} \left(\frac{C_p \, \Delta t_{sub}}{25 \, \lambda} \right) . \qquad (5)$$

The second term of Eq. (1) was evaluated with the conventional Newton cooling law:

$$(\phi_{bo})_{nb} = h_{nb} \, (t_w - t_b)_{bo} \quad , \qquad (6)$$

and $(t_w)_{bo}$ in Eq. (6) was taken from Bernath's generalized plot[2] of $(\Delta t_{sat})_{bo}$ versus T_{sat}/T_c.

Since most nonboiling film-coefficient correlations are written in the form:

$$N_{Nu} = K' \, N_{Re}^m \, N_{Pr}^n \quad , \qquad (7)$$

Eq. (1) may be expressed, by substitution of Eqs. (2) through (7), as:

$$\phi_{bo} = K\lambda\rho_v^{1/2} \, (\sigma g_c a \Delta\rho)^{1/4} \, (F_{sub}) + K' \left(\frac{k}{D_e} \right) N_{Re}^m \, N_{Pr}^n \, (t_w - t_b)_{bo} \quad . \qquad (8)$$

MODIFICATION OF CORRELATION

Available heat-transfer data were examined in order to establish lower limits with which the separate factors of the final correlation could be aligned. It was found that such a fit could be accomplished by selecting an appropriate value of K in Eq. (4) and of K′ in Eq. (7), by altering the subcooling-factor correlation (Eq. 5), and by using a modified plot for the burnout wall superheat.

Specifically, a review of saturated-pool burnout data indicated that for water, a K value of 0.10 is a reasonable minimum. The mean value of K for water is ~0.18 (and for all fluids ~0.15), but variations associated with surface condition and orientation, as well as with the apparently inherent uncertainty (of ~10%) in saturated-pool burnout fluxes,[3] combine to decrease K to a minimum level of ~0.10. For a

$\Delta T_{sat} = T_w - T_{sat}$ $\Delta T_{sat} - \Delta T_{sub} = \Delta T_f$

rough, horizontal heater surface cooled by low-pressure water, the constant K might be as large as 0.20, but for a clean, smooth, long, vertical heater exposed to high-pressure water, K tends toward the lower limit (0.10). $\Delta T_{sub} = T_{sat} - T_{bulk}$

The correlation which best predicts the increase in burnout flux associated with subcooling of the coolant appears to be that of Ivey and Morris,[4] which has the form of Eq. (5) but is based on considerably more extensive data:

$$F_{sub} = 1 + \left(\frac{\rho_\ell}{\rho_v} \right)^{3/4} \left(\frac{C_p \, \Delta t_{sub}}{9.8 \, \lambda} \right) . \tag{9}$$

Since the maximum scatter of the data[4] about Eq. (9) is ~±25%, design values were calculated with:

$$F_{sub,min} = 1 + 0.8 \left(\frac{\rho_\ell}{\rho_v} \right)^{3/4} \left(\frac{C_p \, \Delta t_{sub}}{9.8 \, \lambda} \right) \tag{10}$$

M717

In accord with the forced-convection nonboiling data of Rohsenow and Clark[5] and others, the minimum value of h_{nb} was calculated with the following version of Eq. (7):

.023 use

$$(N_{Nu})_b = 0.019 \, (N_{Re})_b^{0.8} \, (N_{Pr})_b^{1/3} . \tag{11}$$

Calculations were simplified by isolating a combined numerical and physical-property factor from Eq. (11):

$$h_{nb} = F \frac{V^{0.8}}{D_e^{0.2}} , \tag{12}$$

and plotting the factor F, given by:

$$F = 14.4 \frac{k^{2/3} \, C_p^{1/3} \, \rho_\ell^{0.8}}{\mu^{0.467}} , \tag{13}$$

versus bulk water temperature, as shown in Fig. 1. The units of velocity and diameter in this dimensional representation, Eq. (12), must be taken as fps and inches, respectively.

ORNL DWG 68-13462

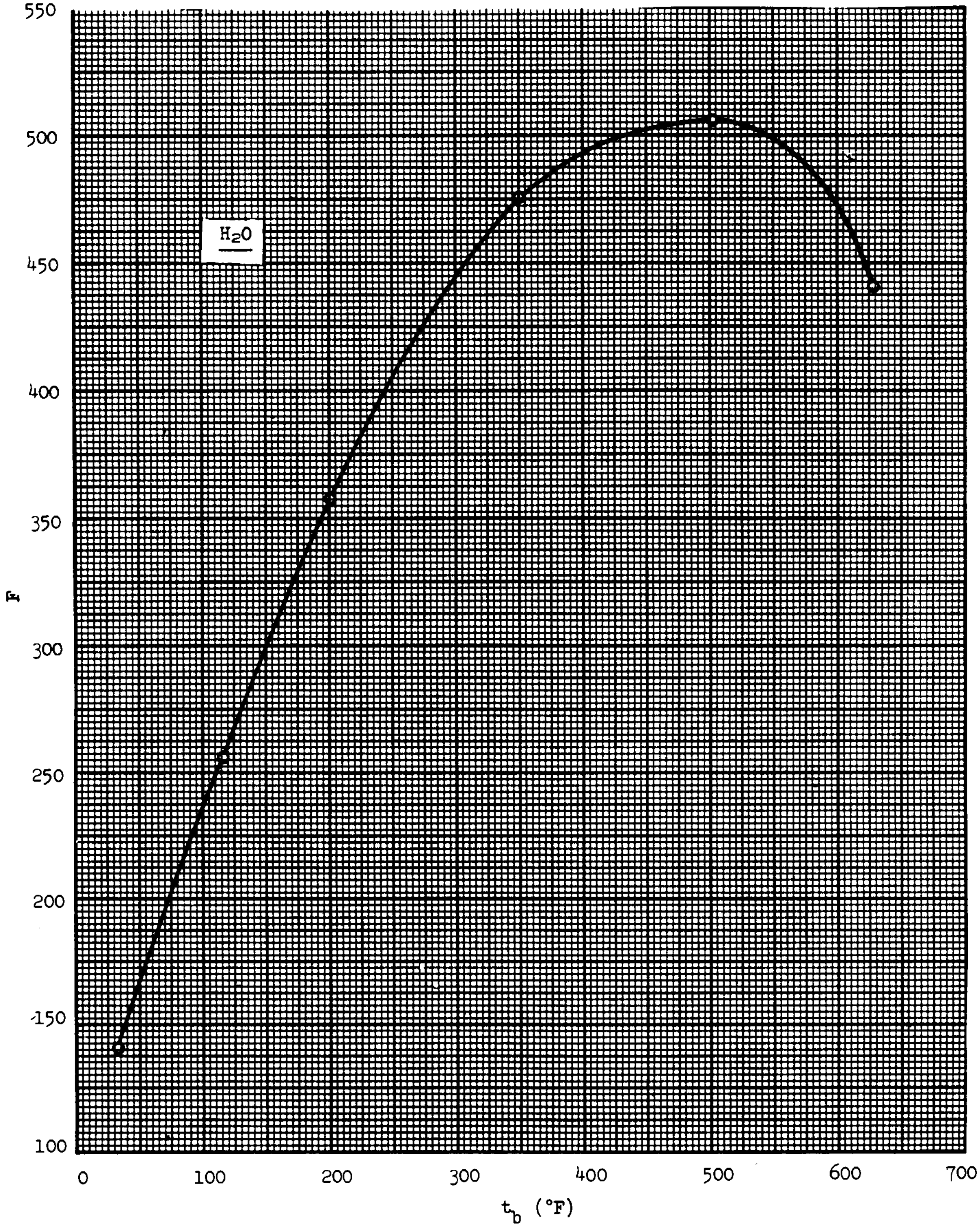

Fig. 1. Variation of Physical-Properties Factor F with Bulk Temperature.

The critical or burnout wall superheat, $(t_w - t_{sat})_{bo}$, enters the calculation since the temperature potential $(t_w - t_b)_{bo}$ in Eqs. (6) and (8) is the sum of the wall superheat and the subcooling at the burnout site, $(t_{sat} - t_b)_{bo}$. The critical superheat varies rather significantly with surface condition, ranging from relatively high values for smooth surfaces with few effective nucleating cavities to small values for rough surfaces. For commercially prepared surfaces, which generally contain a wide range of cavity sizes, the burnout wall superheat has been graphically correlated as a function of P/P_c or of T_{sat}/T_c by Cichelli and Bonilla,[6] Bernath,[2] and Ivey and Morris.[4] Over portions of the pressure range, there is poor agreement among the subject correlations. Bernath's values of $(\Delta t_{sat})_{bo}$, e.g., are, on the average, ~60°F higher than those of Cichelli and Bonilla in the interval $0.2 < (P/P_c) < 1.0$; and behave quite differently at lower reduced pressures, dropping rapidly with pressure reduction rather than rising slowly. In addition, the Ivey and Morris curve gives superheats that are slightly smaller than those shown in the original Cichelli-Bonilla plot.

An overly conservative approach could be taken by ignoring the wall superheat altogether, and using the subcooling as the film temperature difference in Eq. (8). Such a formulation would be contrary to physical reality, however, since the wall superheat must be finite in a boiling system, and the burnout flux with zero subcooling is not zero. In order to take credit for a reasonable value of critical wall superheat, a composite design curve was constructed by combining the correlations of Bernath and of Ivey and Morris, as shown in Fig. 2. The upper (dashed) curves, for $(\Delta t_{sat})_{bo} \leq 68°F$, represent the portions of the subject correlations which lie below their intersection point – i.e., at $t_{sat} < 254°F$, the Bernath curve is lower, whereas for $t_{sat} > 254°F$, the curve of Ivey and Morris gives smaller values of wall superheat. Though there is limited evidence[7] that the Bernath curve is in some error, especially at low pressures, and that the critical wall superheat probably increases with decreasing pressure, as represented by the curve of Ivey and Morris at low t_{sat}, relevant data are too sparse to decide the point conclusively at this time. The design curve (lower solid line of Fig. 2) was taken as

ORNL DWG 68-13463

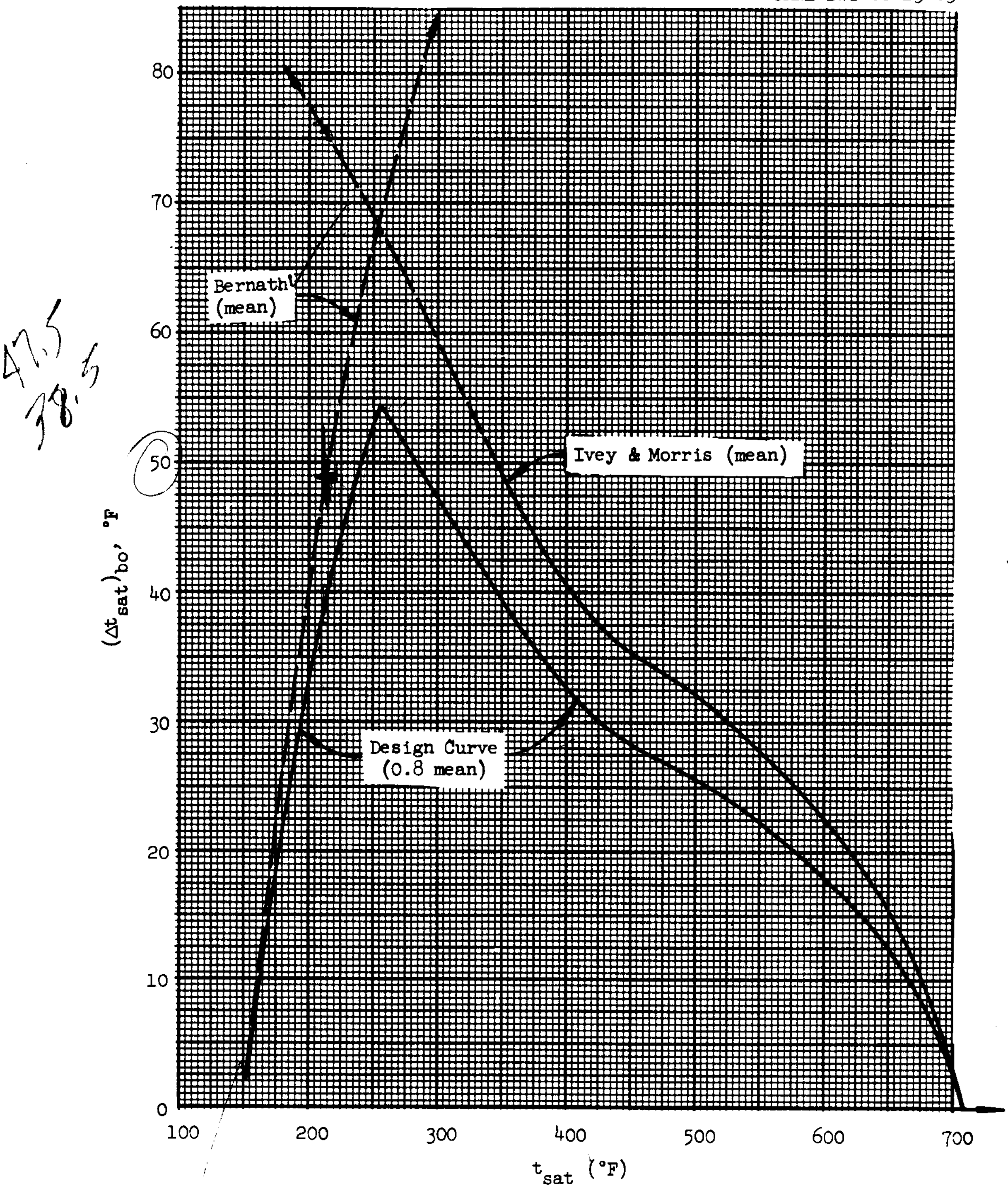

Fig. 2. Variation of Minimum Burnout Wall Superheat with Saturation Temperature for Water.

0.8 of the mean-curve values. The few critical wall-superheat data which have been measured with smooth or commercial surfaces all fall above the design curve.

RESULTS

The calculated minimum burnout fluxes for pool-boiling systems are plotted in Fig. 3 versus pressure, with subcooling as the parameter. Calculated heat fluxes for flow burnout are plotted in Figs. 4 through 11 for coolant velocities of 10 to 100 fps and system pressures of 15, 100, 300, 600, 1000, 1600, 2400, and 3000 psia. In Figs. 5 through 8, corresponding to pressures of 100 to 1000 psia, the high-subcooling curves cross over, their divergence increasing with increasing velocity (at a given pressure) and with decreasing pressure (for fixed subcooling values). The crossover behavior of the curves is attributable to the variation of h_{nb} with bulk temperature – i.e., h_{nb} decreases with decreasing t_b for t_b less than ~500°F (see Fig. 1) – and to the increasing dominance of the forced-convection term as the velocity rises.

Figures 3 through 11 are based on a normal earth gravity ($a/g = 1$), and Figs. 4 through 11 were calculated for $D_e = 0.1$ in. and the ratio $L/D_e \geq 60$. For $L/D_e < 60$, the calculated h_{nb} should be multiplied by the factor $[1 + (D_e/L)^{0.7}]$ to correct for the thermal entry region in which the thermal boundary layer is not fully developed. The forced-convection curves should apply equally well to axial subcooled flows in tubular, annular, and rectangular geometries.

Burnout fluxes for $D_e = 0.5$ in. were also calculated. Figure 12 (parts a through d) displays the results in terms of the ratio of ϕ_{bo} for $D_e = 0.1$ in. to ϕ_{bo} for $D_e = 0.5$ in. plotted versus velocity with subcooling as the parameter. The subject flux ratio varies from 1.06 to 1.34 over the variable ranges investigated. By definition,

$$(\phi_{bo})_{0.5\text{ in.}} = \frac{(\phi_{bo})_{0.1\text{ in.}}}{\text{Fig. 12 ordinate}} \quad . \qquad (14)$$

As discussed previously by the writer,[1] burnout fluxes can be affected significantly by diameters less than a critical value which is

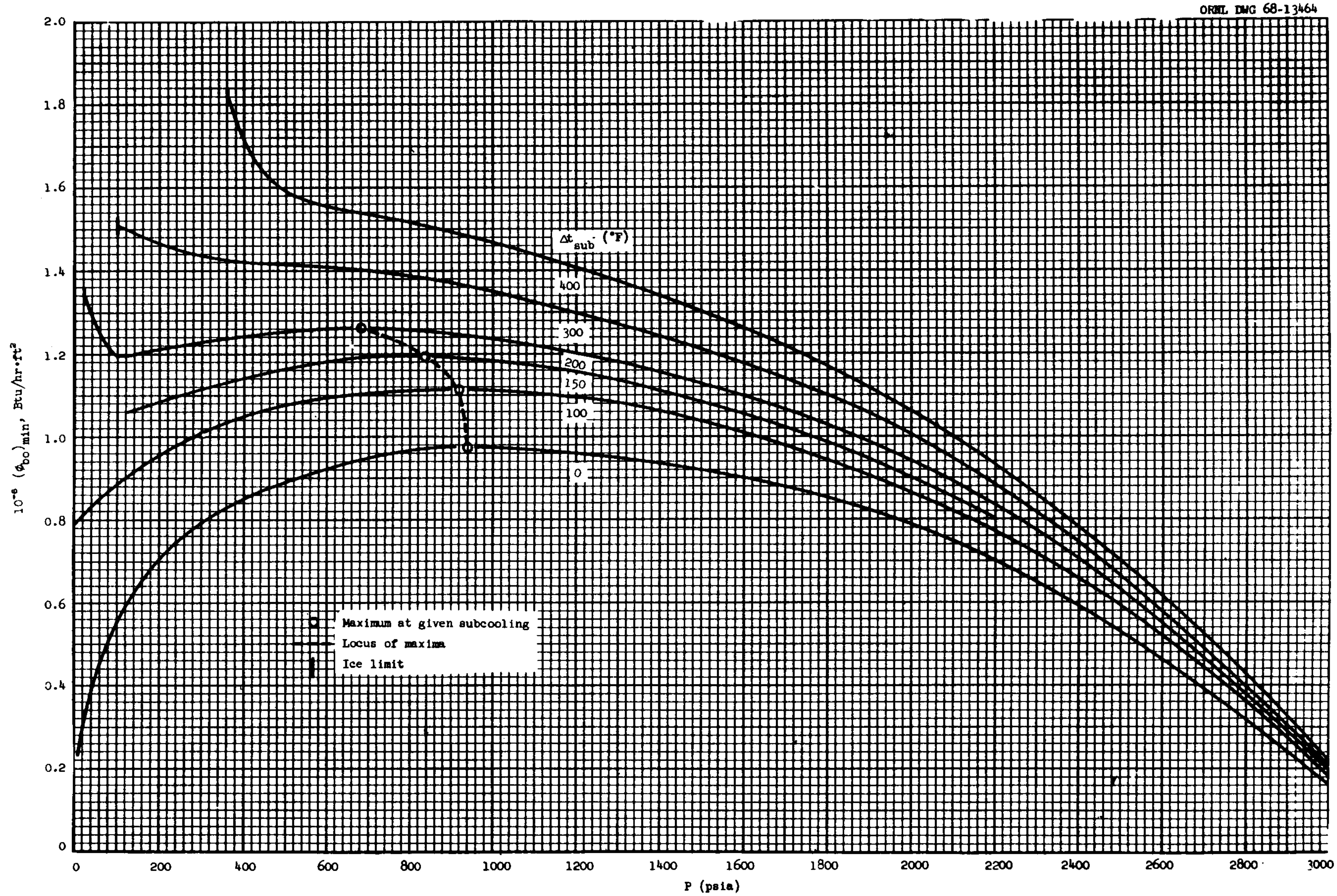

Fig. 3. Pool Boiling of H_2O, Pressure Dependence of Minimum Burnout Heat Flux.

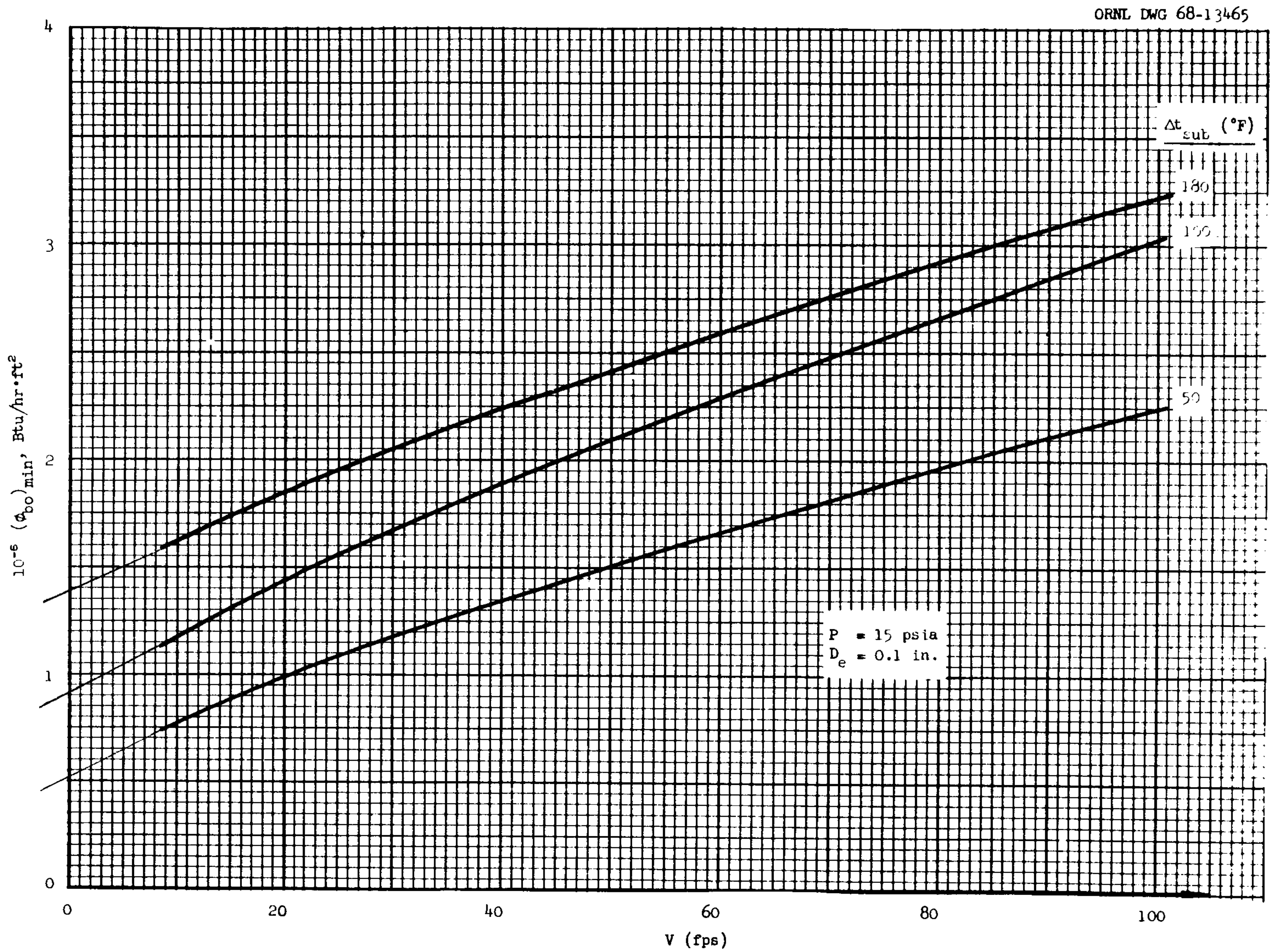

Fig. 4. Forced-Convection Burnout Heat Fluxes, P = 1.0 atm abs.

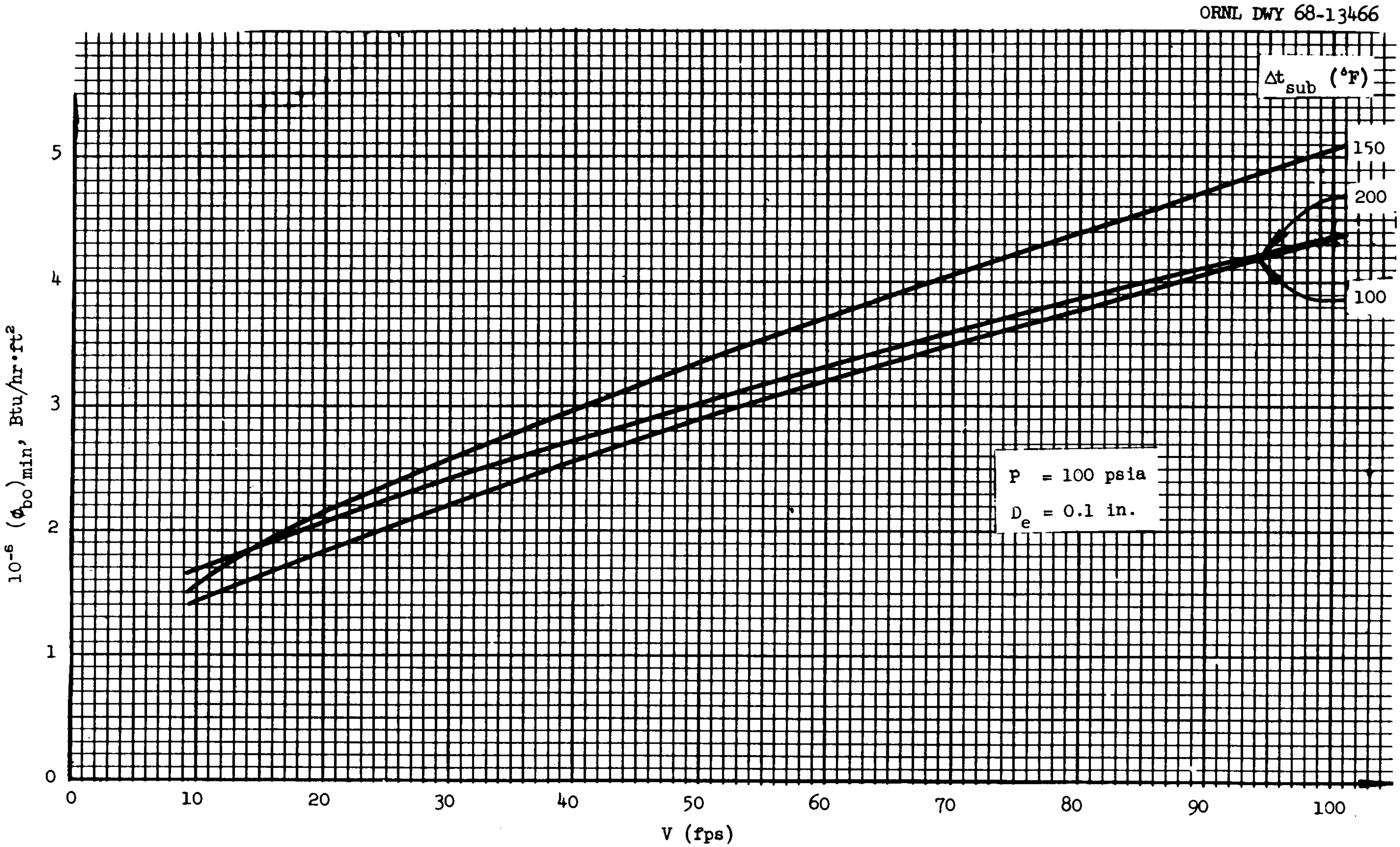

Fig. 5. Forced-Convection Burnout Heat Fluxes, P = 6.8 atm abs.

ORNL DWG 68-13467

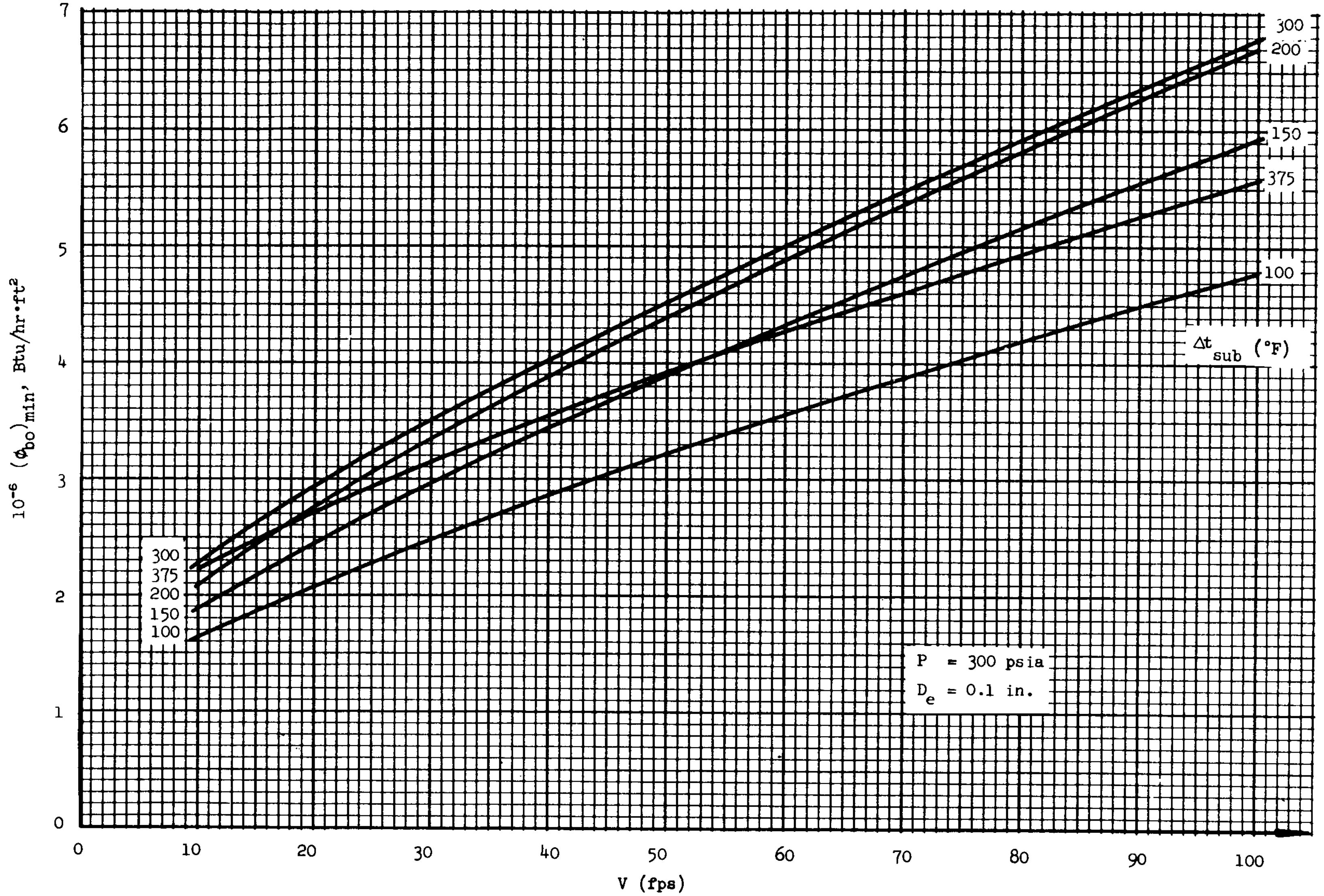

Fig. 6. Forced-Convection Burnout Heat Fluxes, P = 20.4 atm abs.

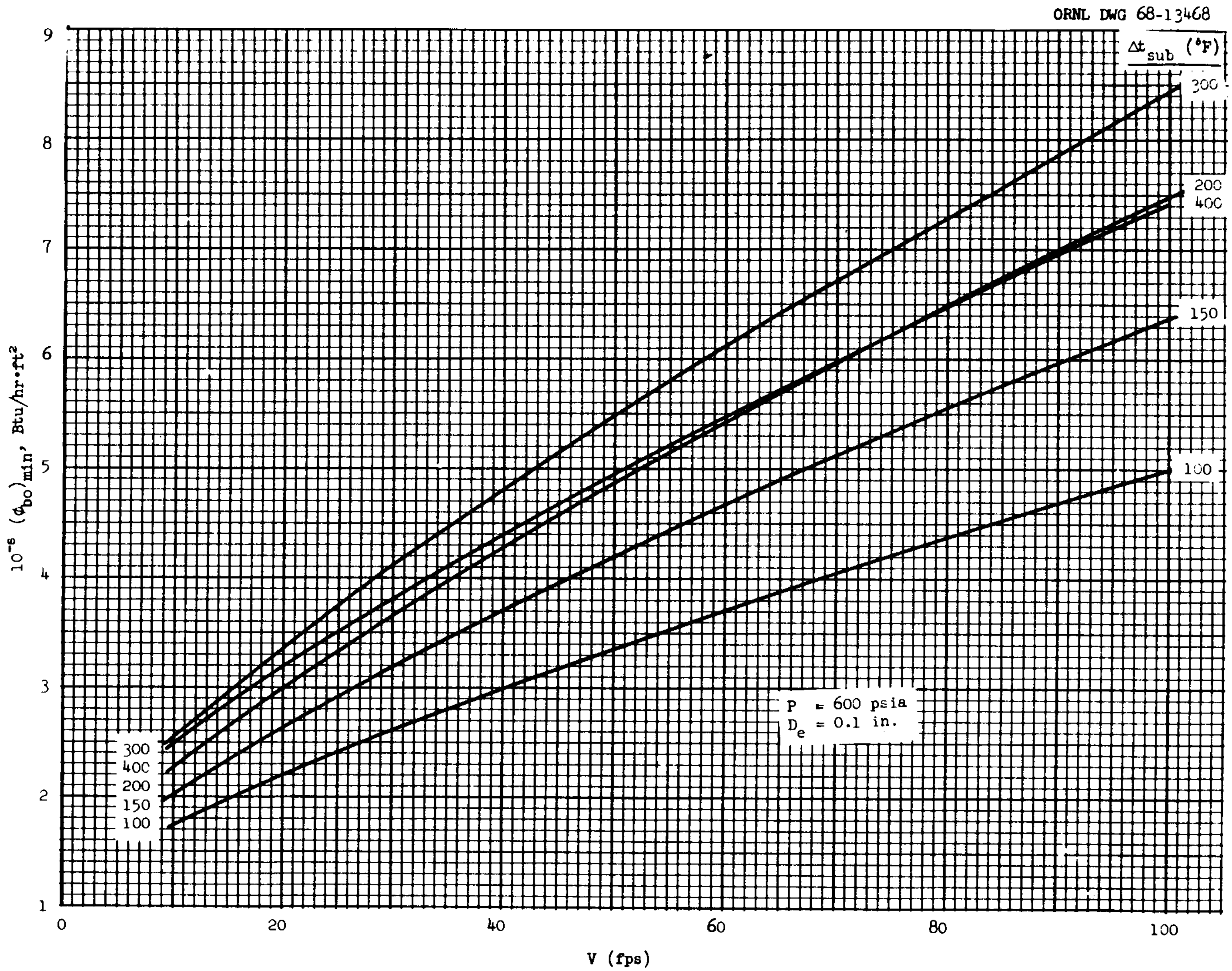

Fig. 7. Forced-Convection Burnout Heat Fluxes, P = 40.8 atm abs.

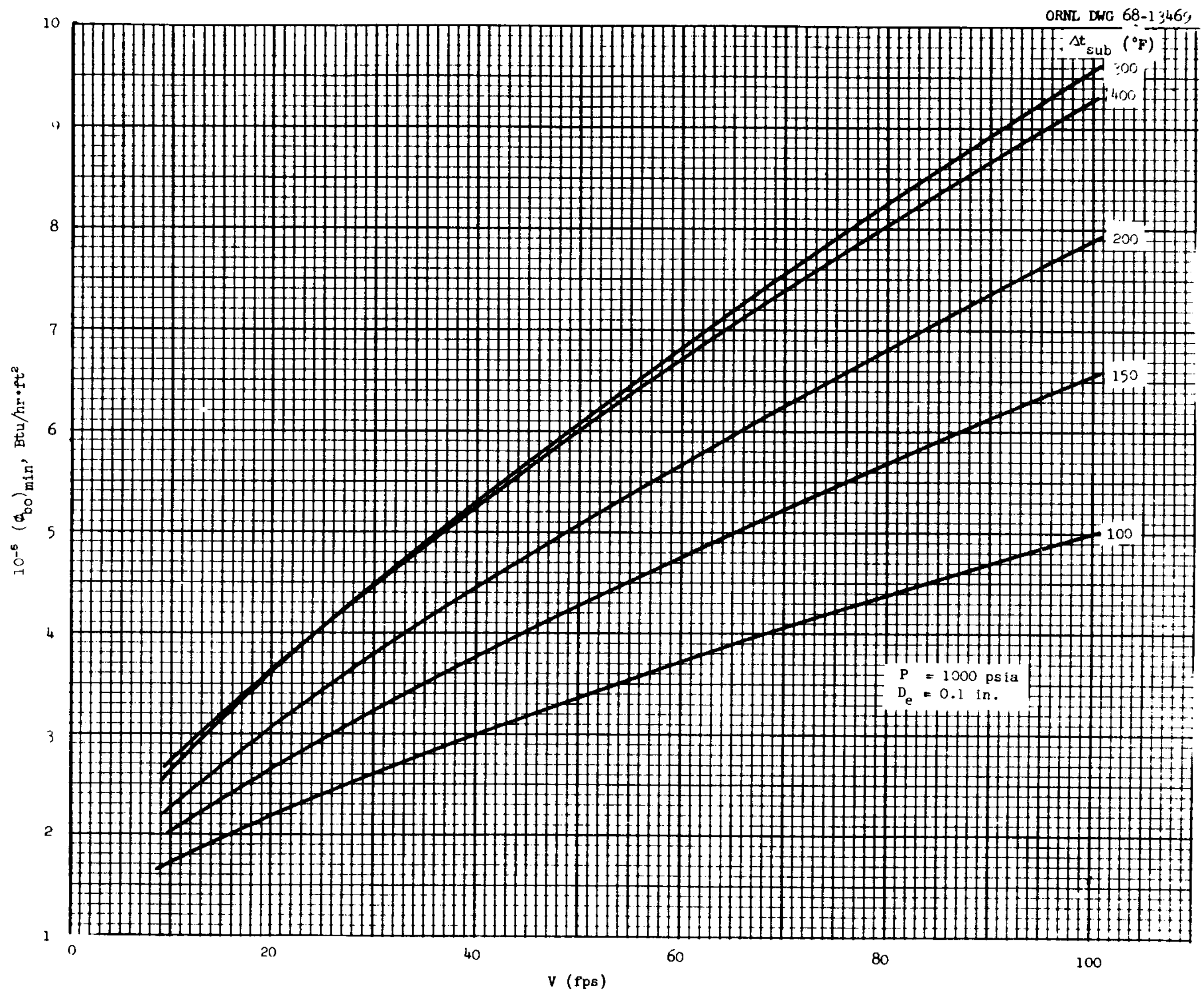

Fig. 8. Forced-Convection Burnout Heat Fluxes, P = 68.0 atm abs.

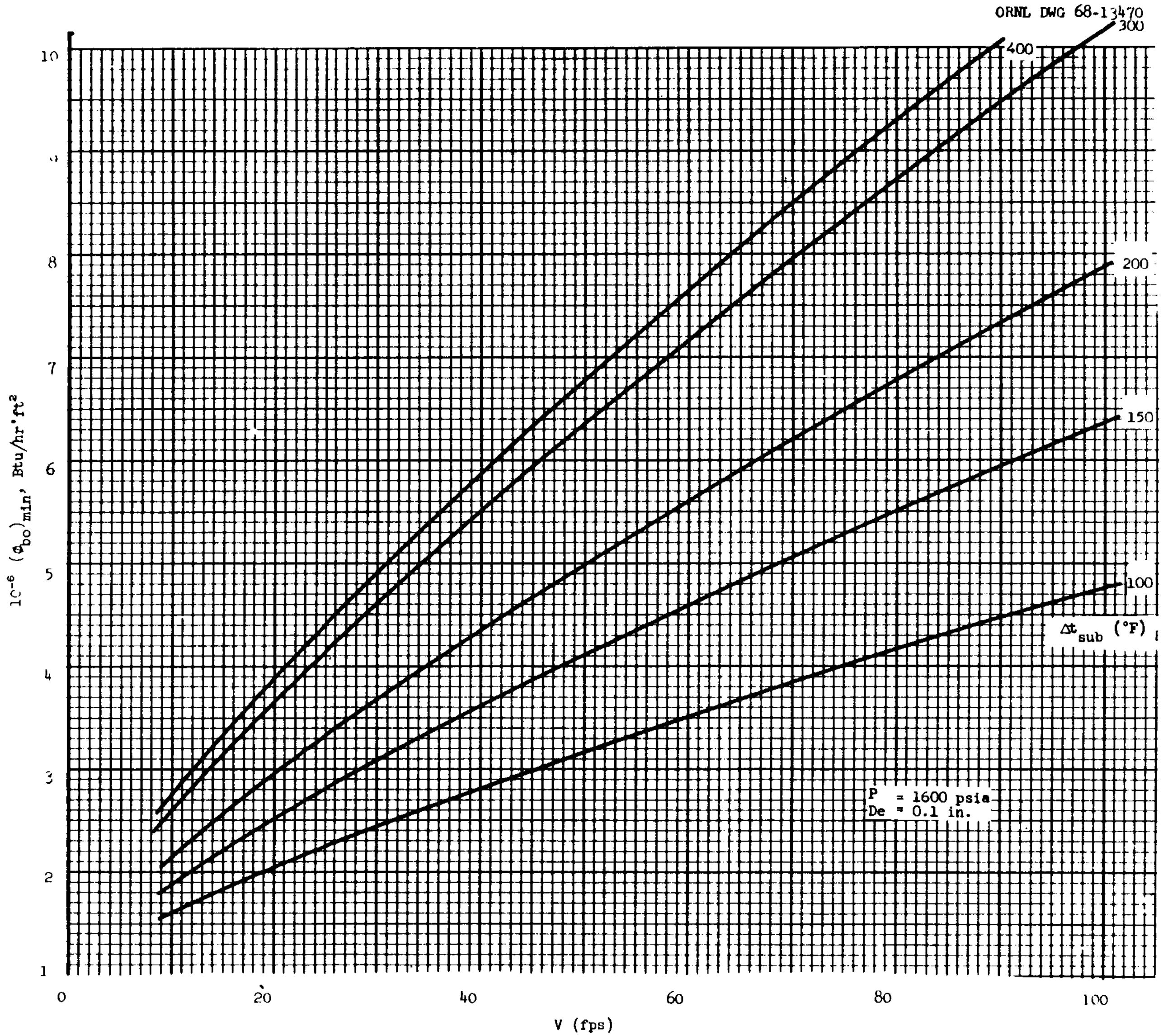

Fig. 9. Forced-Convection Burnout Heat Fluxes, P = 108.9 atm abs.

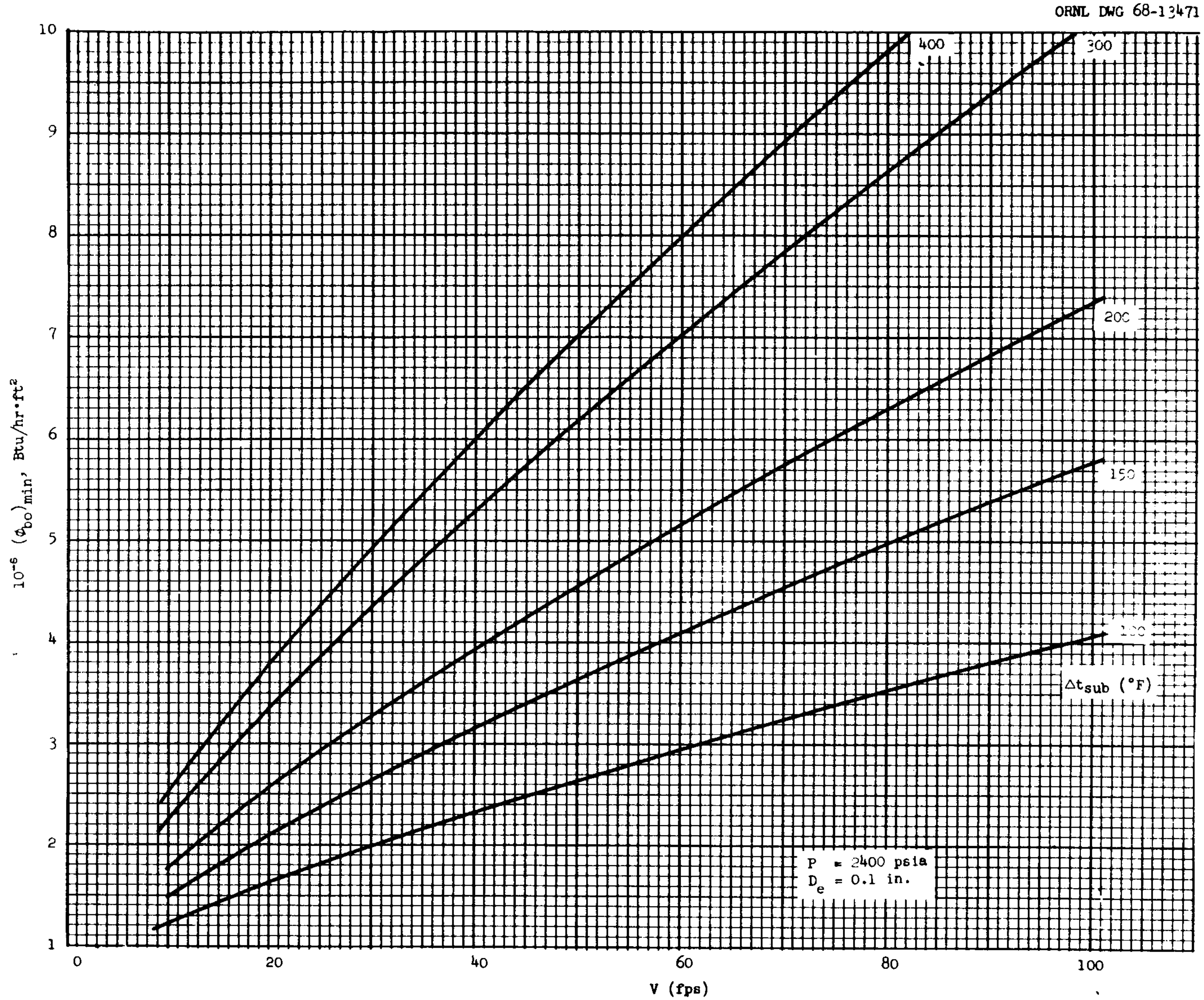

Fig. 10. Forced-Convection Burnout Heat Fluxes, P = 163.3 atm abs.

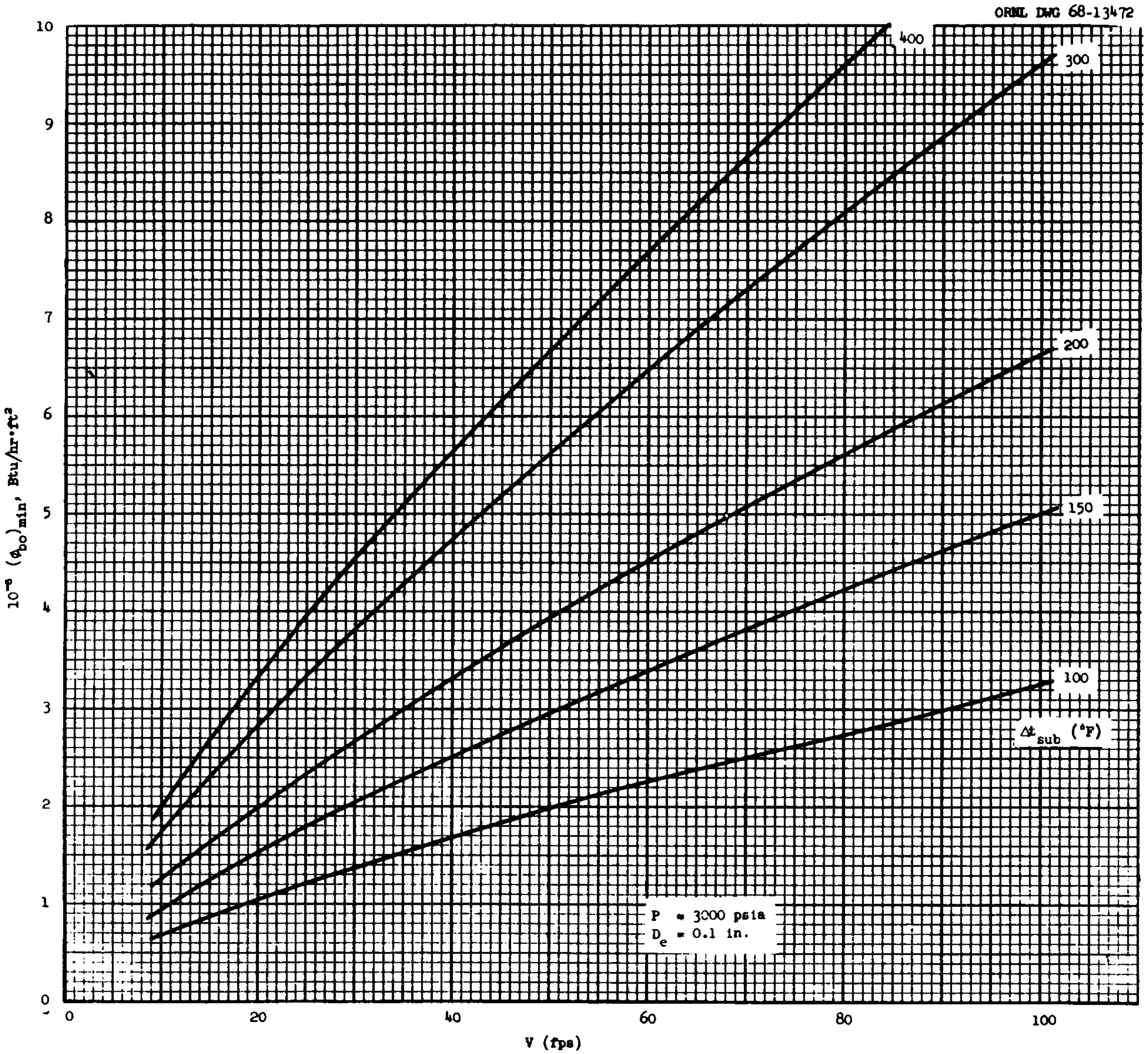

Fig. 11. Forced-Convection Burnout Heat Fluxes, P = 204.1 atm abs.

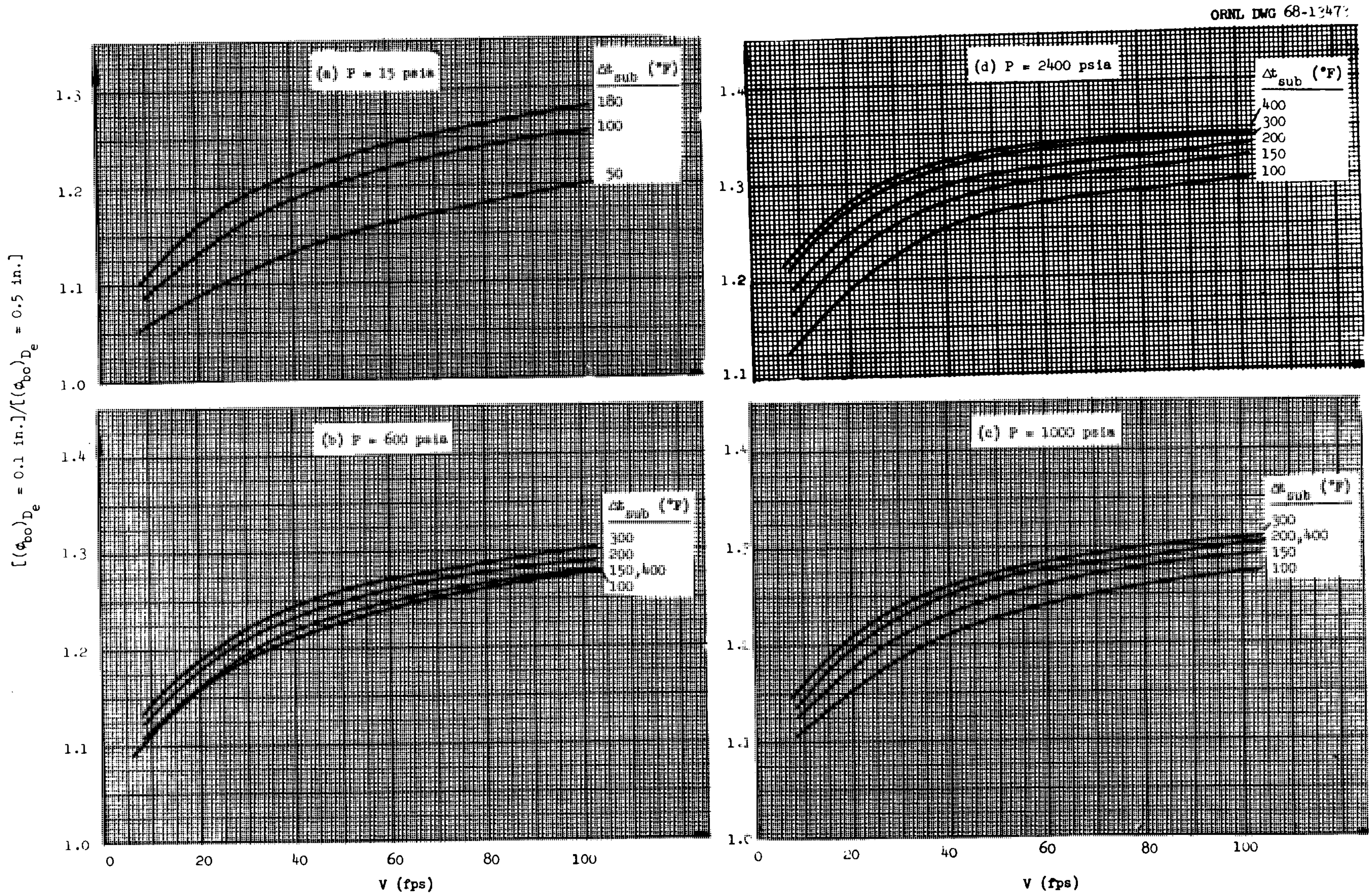

Fig. 12. Dependence of Ratio of Burnout Fluxes for Two Diameters on Velocity, Subcooling, and Pressure.

comparable to bubble dimensions. The limited data acquired with sufficiently confined geometries indicate that for water, the "critical" diameter varies with pressure approximately as follows:

P (atm abs) →	1	30	90	150	200
$(D_e)_c$, mils →	75	58	45	36	20

If $D_e < (D_e)_c$, the design curves are not applicable, since the burnout fluxes will be either sharply increased or decreased, depending on the hydraulic supply-demand characteristics of the system.

CALCULATING THE RATIO OF BURNOUT TO INCIPIENT-BOILING HEAT FLUXES

The amount by which a local heat flux, ϕ_x, can be increased beyond first boiling ($\phi_x = \phi_{ib}$) before burnout occurs ($\phi_x = \phi_{bo}$) is frequently desired in reactor safety analyses. The subscript "x" is used to emphasize that an increase in the local heat flux only is under consideration. If the total channel power is increased significantly, the burnout flux is decreased because the increased upstream heat load decreases the local subcooling at the burnout site.

The heat flux ϕ_{ib} can be calculated by simultaneously solving Eq. (6) in the form:

$$\phi_{nb} = h_{nb} \, (\Delta t_{sat} + \Delta t_{sub}) , \tag{15}$$

with the dimensional expression proposed for water by Bergles and Rohsenow:[8]

$$(\phi_{ib})_{locus} = 15.6 \, P^{1.156} \, (\Delta t_{sat})^{2.30/P^{0.0234}} , \tag{16}$$

15.29 for D.O

in which the appropriate units are Btu/hr•ft², psia, and °F.

An alternative approach is based on an interpretation of the method of superposition as illustrated by Fig. 13, in which the line AB corresponds to nonboiling convective heat transfer, the line BC to the nucleate-boiling region, the point C to the critical (burnout) condition, and extensions CE and CF to the course of the boiling curve, for $\Delta t_{sat} > (\Delta t_{sat})_c$, when the heat source is one of constant heat flux and of constant temperature, respectively. Since the slope of AD is small, and $(\Delta t_{sat})_{to}$ is not

ORNL DWG 68-13474

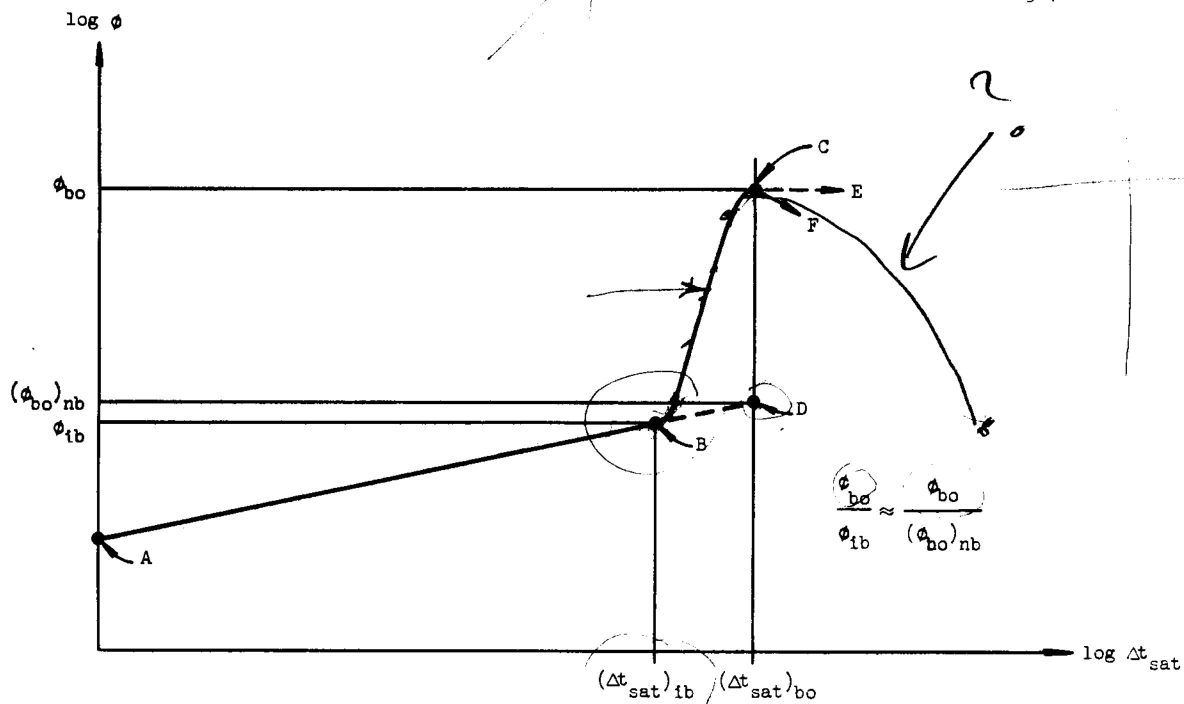

Fig. 13. Illustration of Method of Calculating the Ratio of Burnout to Incipient-Boiling Heat Fluxes.

much larger than $(\Delta t_{sat})_{ib}$, and since $(\phi_{bo})_{nb}$ as defined in the additive correlation [Eq. (6)] corresponds to point D, it follows that $\phi_{ib} \approx (\phi_{bo})_{nb}$ and that:

$$\frac{\phi_{bo}}{\phi_{ib}} \approx \frac{\phi_{bo}}{(\phi_{bo})_{nb}} = \frac{\text{Eq. (8)}}{\text{Eq. (6)}} \quad . \tag{17}$$

As is clear from Fig. 13, the ratio ϕ_{bo}/ϕ_{ib} should be slightly underpredicted by this procedure.

For a nominal HFIR case ($P = 600$ psia, $V = 45$ fps, $D_e = 0.1$ in., and $\Delta t_{sub} = 250°F$), the flux ϕ_{ib} as calculated by simultaneous solution of Eqs. (15) and (16) gives a ratio ϕ_{bo}/ϕ_{ib} of 1.442. The prediction of Eq. (17), 1.385, is only 4% smaller. These calculations have been extended to show, in Fig. 14, the velocity, subcooling, and pressure dependencies of the ϕ_{bo}/ϕ_{ib} ratio for base values of $V = 45$ fps, $\Delta t_{sub} = 200°F$, and $P = 600$ psia.

CONCLUSIONS

Design curves of burnout heat flux for subcooled water systems were based on $K = 0.10$ (2/3 overall mean value), $K' = 0.019$ (0.8 mean value), $(\Delta t_{sat})_c = 0.8$ of probable minimum value, and subcooling-factor increment = mean/1.25. The plotted curves should be valid for diameters above a critical value which varies with system pressure.

A simple method of estimating the ϕ_{ib} is proposed; based on limited comparisons, the method gives good agreement with the procedure of Bergles and Rohsenow.

ACKNOWLEDGMENT

The writer wishes to express his appreciation to J. Lones, project technician, for his assistance with the calculations and curve plotting.

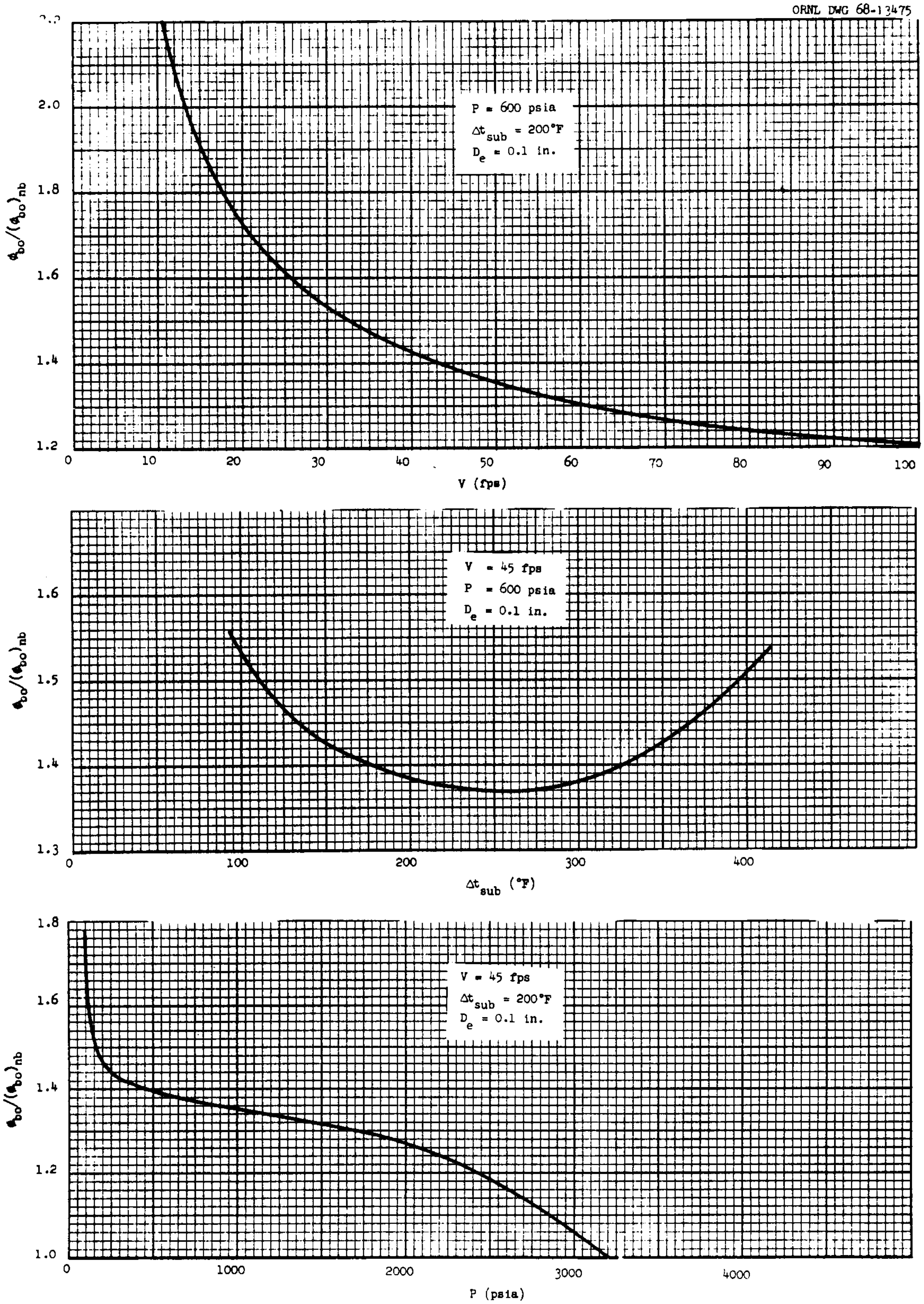

Fig. 14. Variation of the Ratio of Burnout to Incipient-Boiling Heat Fluxes as Predicted by the Additive Method (Fig. 13) -- Nominal HFIR Conditions.

ADDENDUM

In a recent comparison of burnout correlations for water coolant,[9] it was shown that a dimensionless equation developed by Kutateladze[10] for the case of a high-velocity just-saturated liquid:

$$\phi_c = 0.0155\, V\lambda\, (\rho_\ell\, \rho_v)^{1/2}\, N_{Re}^{-1/5}\ , \tag{18}$$

is in excellent agreement at the higher velocities with the superposition correlation, Eq. (8), as modified. With Eq. (18), $\phi_c \rightarrow 0$ as $V \rightarrow 0$; and at $V = 0$, the difference between the predictions of Eqs. (8) and (18) is essentially the value of ϕ_c for the saturated-pool case.

It is also noted in Ref. 9 that buoyancy forces in heated vertical channels cooled by low-velocity downflows act to decrease the ϕ_c significantly below corresponding values in upflow or horizontal-flow systems. In normally encountered geometries, this effect is negligible for water when V exceeds about 8 fps. The velocity below which the buoyancy effect is important increases with increasing L/D_e; for values of this ratio less than about 200, the buoyancy correction is negligible for $V \geq 10$ fps.[11]

NOTATION

a	system acceleration
C_p	constant-pressure specific heat of liquid
D_e	equivalent diameter of flow channel
F	liquid physical-properties factor [see Eq. (13)]
F_{sub}	subcooling factor [see Eq. (3)]
G	mass velocity of coolant
g	gravitational acceleration
g_c	mass-to-force conversion constant
h	heat-transfer coefficient
k	thermal conductivity of liquid
K	constant [Eq. (4)]
K'	constant [Eq. (7)]
L	heated length
m, n	constant exponents, 0.8 and 1/3, respectively
N_{Nu}	Nusselt modulus, dimensionless, hD_e/k
N_{Pr}	Prandtl modulus, dimensionless, $C_p\mu/k$
N_{Re}	Reynolds modulus, dimensionless, D_eG/μ
P	absolute system pressure
P_c	thermodynamic critical pressure
t	temperature
T_c	thermodynamic critical temperature
T_{sat}	absolute saturation temperature
Δt_{sat}	wall superheat, $(t_w - t_{sat})$
Δt_{sub}	coolant subcooling, $(t_{sat} - t_b)$
V	axial coolant velocity

Greek Letters

λ	latent heat of vaporization
μ	dynamic viscosity of liquid
ρ	density
$\Delta\rho$	phase density difference, $(\rho_{\ell} - \rho_v)$
σ	surface tension, liquid/vapor
ϕ	heat flux

Subscripts

b	bulk (mixed mean)
bo	burnout
boil	boiling
c	critical
ib	incipient boiling
ℓ	of liquid
min	minimum
nb	nonboiling
sat	saturation
sub	subcooled
v	of vapor
w	wall
x	local

LITERATURE CITED

1. W. R. Gambill, Generalized Prediction of Burnout Heat Flux for Flowing, Subcooled, Wetting Liquids, Chem. Eng. Progr. Symposium Series, 59(41): 71–87 (1963); also USAEC Report TID-7642, 112–137, 1963.

2. L. Bernath, A Theory of Local Boiling Burnout and Its Application to Existing Data, Chem. Eng. Progr. Symposium Series, 56(30): 95–116 (1960).

3. W. R. Gambill, An Experimental Investigation of the Inherent Uncertainty in Pool Boiling Critical Heat Fluxes to Saturated Water, A.I.Ch.E. Journal, 10(4): 502–508 (July 1964).

4. H. J. Ivey and D. J. Morris, On the Relevance of the Vapor-Liquid Exchange Mechanism for Sub-Cooled Boiling Heat Transfer at High Pressure, British Report AEEW-R 137, Fig. 4, January 1962.

5. W. M. Rohsenow and J. A. Clark, Heat Transfer and Pressure Drop Data for High Heat Flux Densities to Water at High Sub-Critical Pressures, pp. 193–207 in 1951 Heat Transfer and Fluid Mechanics Institute, Stanford University Press, Stanford, California, 1951.

6. M. T. Cichelli and C. F. Bonilla, Heat Transfer to Liquids Boiling under Pressure, Trans. Am. Inst. Chem. Engrs., 41: 755–787 (1945).

7. H. L. Wessel, Investigation of Forced-Convection Subcooled Boiling, S.B. thesis in Mechanical Engineering, Massachusetts Institute of Technology, Cambridge, Massachusetts, May 1964.

8. A. E. Bergles and W. M. Rohsenow, The Determination of Forced-Convection Surface-Boiling Heat Transfer, J. Heat Transfer, 86: 365–372 (1964).

9. W. R. Gambill, Burnout in Boiling Heat Transfer – Part II: Subcooled Forced-Convection Systems, Nuclear Safety, 9(6): 467–480 (November-December 1968).

10. S. S. Kutateladze, Criteria of Stability in Two-Phase Flow, pp. 83–92 in Symposium on Two-Phase Flow, Vol. 1, University of Exeter, Devon, England, June 1965.

11. W. R. Gambill, unpublished results; continuation of the study of Ref. 56 cited in Ref. 9.

INTERNAL DISTRIBUTION

1. L. G. Alexander
2. S. E. Beall
3. R. H. Chapman
4. T. G. Chapman
5. R. D. Cheverton
6. H. C. Claiborne
7. T. E. Cole
8. J. W. Cooke
9. W. B. Cottrell
10. B. Cox
11. F. L. Culler
12. J. A. Dahlheimer
13. D. M. Eissenberg
14. D. E. Ferguson
15. A. P. Fraas
16-27. W. R. Gambill
28. L. A. Haack
29. P. N. Haubenreich
30. H. W. Hoffman
31. J. K. Jones
32. J. D. Joyner
33. P. R. Kasten
34. J. J. Keyes, Jr.
35. G. J. Kidd, Jr. (ORGDP)
36. O. H. Klepper
37. C. G. Lawson
38. M. I. Lundin
39. R. N. Lyon
40. R. E. MacPherson
41. H. C. McCurdy
42. A. J. Miller
43. A. M. Perry
44. M. W. Rosenthal
45. G. Samuels
46. W. K. Sartory
47. A. W. Savolainen
48. J. D. Sheppard
49. M. J. Skinner
50. I. Spiewak
51. D. A. Sundberg
52. D. G. Thomas
53. D. B. Trauger
54. J. N. Turpin (Y-12)
55. C. C. Webster
56. G. D. Whitman
57. R. P. Wichner
58. M. M. Yarosh
59-60. Central Research Library (CRL)
61-62. Y-12 Document Reference Section (DRS)
63-65. Laboratory Records Department (LRD)
66. Laboratory Records Department — Record Copy (LRD-RC)

EXTERNAL DISTRIBUTION

67-81. Division of Technical Information Extension (DTIE) – [illegible]
82. Laboratory and University Division, ORO
83. J. E. Mott, Nuclear Engineering Department, University of Tennessee
84-350. **Given distribution as shown in TID-4500 (52nd ed.) under Reactor Technology (25 copies - CFSTI)**